Università degli Studi di Napoli "Federico II"

SCUOLA POLITECNICA E DELLE SCIENZE DI BASE

DIPARTIMENTO DI INGEGNERIA INDUSTRIALE

CORSO DI LAUREA IN INGEGNERIA AEROSPAZIALE

CLASSE DELLE LAUREE IN INGEGNERIA INDUSTRIALE (L-9)

Elaborato di laurea in Meccanica del Volo

Aircraft performance and static stability analysis with MATLAB live script

Relatore:
Prof. Danilo Ciliberti

Candidato:
Antonio Russano
Matr. N35003530

ANNO ACCADEMICO 2021 – 2022

Alla mia famiglia e a coloro che
mi hanno insegnato a guardare in alto.
Remember to look up at the stars
and not down at your feet.
(Stephen Hawking)

Abstract

This report is divided in three parts:

1) The first part shows the influence of the elevator on the trend of the $C_L - \alpha$ and $C_M - \alpha$ curves, for a fixed value of i_h.
2) The second part shows a representation of the wing in plan and from the front by the variation of the following value:
   - Aspect ratio AR
   - Taper ratio λ
   - Sweepback Λ_{le}
   - Dihedral angle Γ

   Then some coefficients relating to lateral and directional stability are determined.
3) The third part shows the ideal range of an electric aircraft by the variation of the following parameters:
   - Battery specific energy E^*
   - Lift to drag ratio $\frac{L}{D}$
   - Propulsion efficiency η_{tot}
   - Mass battery fraction $\frac{m_{batt}}{m}$

   For all these parts it is implemented a code for MATLAB LIVE SCRIPT.

Sommario

Questa relazione è divisa in tre parti:

1) La prima parte mostra l'effetto dell'elevatore sulle curve $C_L - \alpha$ e $C_M - \alpha$ per un valore fisso di i_h.
2) Nella seconda parte è mostrata l'ala in pianta e frontalmente attraverso la variazione dei seguenti parametri:
   - Allungamento alare AR
   - Rapporto di rastremazione λ
   - Angolo di freccia Λ_{le}
   - Angolo di diedro Γ

   Successivamente sono calcolati alcuni coefficienti relativi alla stabilità direzionale.
3) Nella terza parte è mostrato il calcolo semplificato del range di un velivolo elettrico attraverso la variazione dei seguenti parametri
   - Energia specifica batteria E^*
   - Efficienza aerodinamica $\frac{L}{D}$
   - Efficienza propulsiva η_{tot}
   - Frazione di massa batteria $\frac{m_{batt}}{m}$

Per tutte queste parti è stato implementato un codice per MATLAB LIVE SCRIPT.

Table of contents

List of figures

Introduction

In order to study the behavior of an aircraft, it is necessary to establish an important concept: the stability.

A system is stable if, after an external perturbation, it tends to return to the initial configuration state.

Thus, if a system, in equilibrium state, returns to equilibrium following a small disturbance, the state is said to be a stable equilibrium.

As concern flight controls, the elevators are the movable parts of the horizontal tail, allowing pitch control. To perform a nose-up pitching maneuver, these move symmetrically upwards, decreasing the lift on the tail. They are controlled by the longitudinal movement of the pilot stick.

It is possible to study the effect that the elevator has on the lift curve vs. the angle of attack $C_L - \alpha$ and on the pitching moment coefficient curve vs. the angle of attack $C_M - \alpha$.

If the airplane is longitudinally stable, a change in the elevator angle δ_e will change the angle of attack α such that the pitching moment coefficient is $C_M = 0$; the α_{eq} (such that $C_M = 0$) is identified on the $C_M - \alpha$ curve.

It is possible to obtain the value of the angle α from the $C_L - \alpha$ curves with the values of C_L in the characteristic points of the drag polar and, through the variation of δ_e, it is possible to move the $C_M - \alpha$ curves in correspondence of $C_M = 0$ to the α value.

It is possible to define other important variables, in particular:

- The wing pitching moment coefficient $C_{M_{ac}}$
- The contribution of the wing due to the sweepback to the yaw moment coefficient C_{N_β}
- The wing contribution to the dihedral effect due to the sweepback $C_{l_{\beta,\Lambda}}$
- The wing contribution to the dihedral effect due to the dihedral angle $C_{l_{\beta,\Gamma}}$

Through a code in MATLAB LIVE SCRIPT is possibile to represent a wing in which we can set the value of:

- Aspect ratio AR
- Taper ratio λ
- Sweepback Λ_{le}
- Dihedral angle Γ

Thus, with these parameters, for every wing we can estimate the value of the stability coefficients and then represent the variation of the $C_{M_{ac}}$ and $C_{L_{\alpha,w}}$whit the aspect ratio AR and the variation of C_{N_β}, $C_{l_{\beta,\Lambda}}$ and $C_{l_{\beta,\Gamma}}$ with C_L at different values of the sweep angle Λ_{le}.

1. Influence of elevator

1.1 Parabolic drag polar

The parabolic drag polar is an approximation of the real polar in the $C_L - C_D$ plane.

For the determination of this curve this expression of C_D is used:

$$C_D = C_{D_0} + \frac{{C_L}^2}{eAR\pi}; \quad (1)$$

where:

- AR is the aspect ratio
- C_{D_0} is the drag coefficient at zero lift.
- e is the Oswald's factor

1.2 Characteristic points

In this part the characteristic points E, A and P are calculated on the parabolic drag polar.

1.2.1 Point E

For the determination of the point E, which represents the point of maximum aerodynamic efficiency for all the airplanes and the condition of the (theoretical) maximum range for a propeller-driven aircraft, we use these relations:

$$C_{L_E} = \sqrt{\pi AR C_{D_0} e}; \quad (2)$$

$$C_{D_E} = 2C_{D_0}; \quad (3)$$

1.2.2 Point A

For the determination of the point A, which represents the condition of maximum range for a jet aircraft, we use these relations:

$$C_{L_A} = \frac{C_{L_E}}{\sqrt{3}}; \quad (4)$$

$$C_{D_A} = \frac{4}{3} C_{D_0}; \quad (5)$$

1.2.3 Point P

For the determination of the point P, which represents the condition of minimum power for all the airplanes and the maximum endurance for propeller-driven aircraft, we use these relations:

$$C_{L_P} = \sqrt{3} C_{L_E}; \quad (6)$$

$$C_{D_P} = 4 C_{D_0}; \quad (7)$$

1.3 Lift coefficient

In the first approach, for estimate the $C_L - \alpha$ curves and for the study of the variation of this curve by varying the value of δ_e, we can linearize the expression of C_L.

In particular:

$$C_L = C_{L_0} + C_{L_\alpha} \alpha + C_{L_{\delta e}} \delta_e + C_{L_{i_h}} i_h; \quad (8)$$

In this way we can express C_L as a function of α and the parameter that changes is δ_e.

1.4 Pitching moment coefficient

Like the lift coefficient, for the study of the variation of the $C_M - \alpha$ curves by varying the value of $\delta_e$we can linearize the expression of C_M.

In particular:

$$C_M = C_{M_0} + C_{M_\alpha} \alpha + C_{M_{\delta_e}} \delta_e + C_{M_{i_h}} i_h; \quad (9)$$

Like the C_L, In this way we can express C_M as a function of α and the parameter that changes is again δ_e.

1.5 Graphic representation

In the following diagrams we can see the polar parabolic (in which is neglecting the effect of the deflection of the elevator) and the $C_L - \alpha$, $C_M - \alpha$ curves at different value of δ_e

We can assume for the problem this set of data:

```
n              =  30;                          %point number
v              =  ones(n,1);
%DATA
Cl_0w          =  0.228*v;
Cl_a           =  0.09;                        %[deg^-1]
Cl_ih          =  0.0135;                      %[deg^-1]
Cl_de          =  0.0065;                      %[deg^-1]
CL             =  linspace(0,1.5,n)';
ih             = -2*v;                         %[deg]
CM_0           = -0.0622*v;
CM_a           = -0.0166;                      %[deg^-1]
CM_ih          = -0.0401;                      %[deg^-1]
CM_de          = -0.0192;                      %[deg^-1]
CD_0           =  0.032;
e              =  0.78;
AR             =  9.75;
```

Figure 1 – Data of the problem

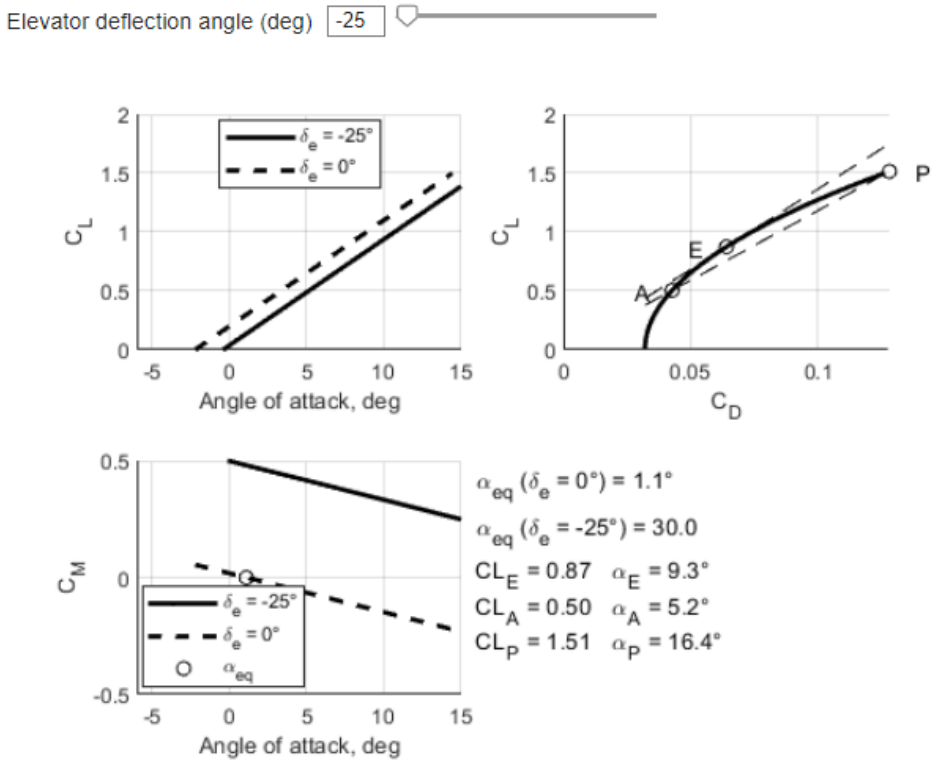

Figure 2 – Parabolic drag polar, $C_L - \alpha$ and $C_M - \alpha$ curves at $\delta_e = -25°$

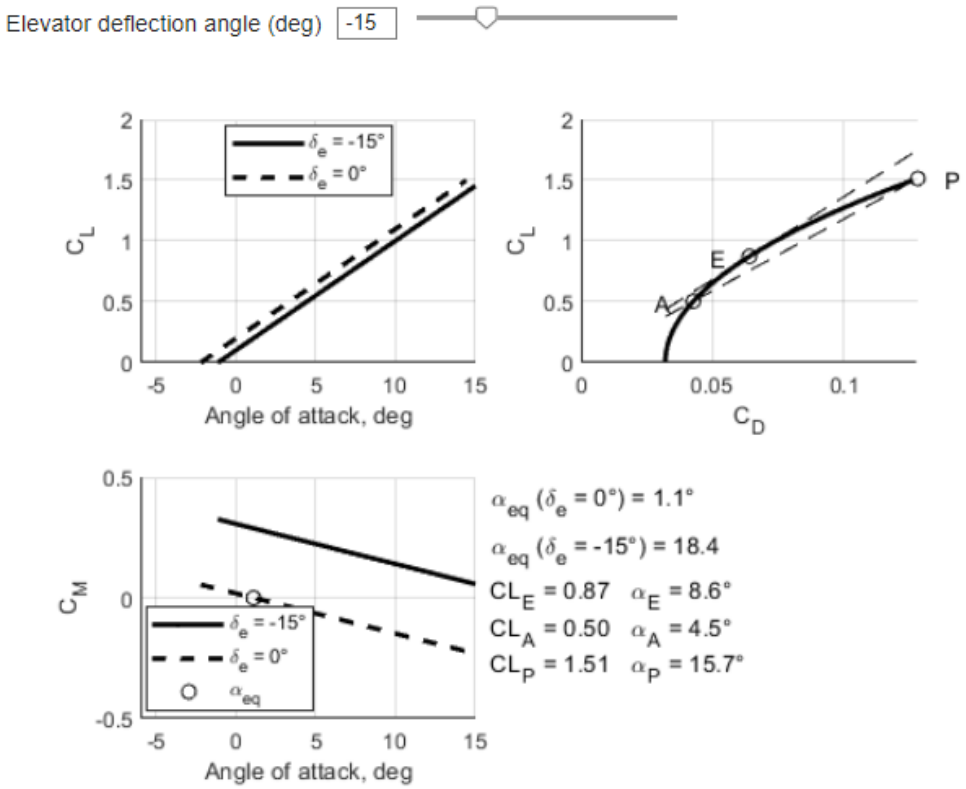

Figure 3 – Parabolic drag polar, $C_L - \alpha$ and $C_M - \alpha$ curves at $\delta_e = -15°$

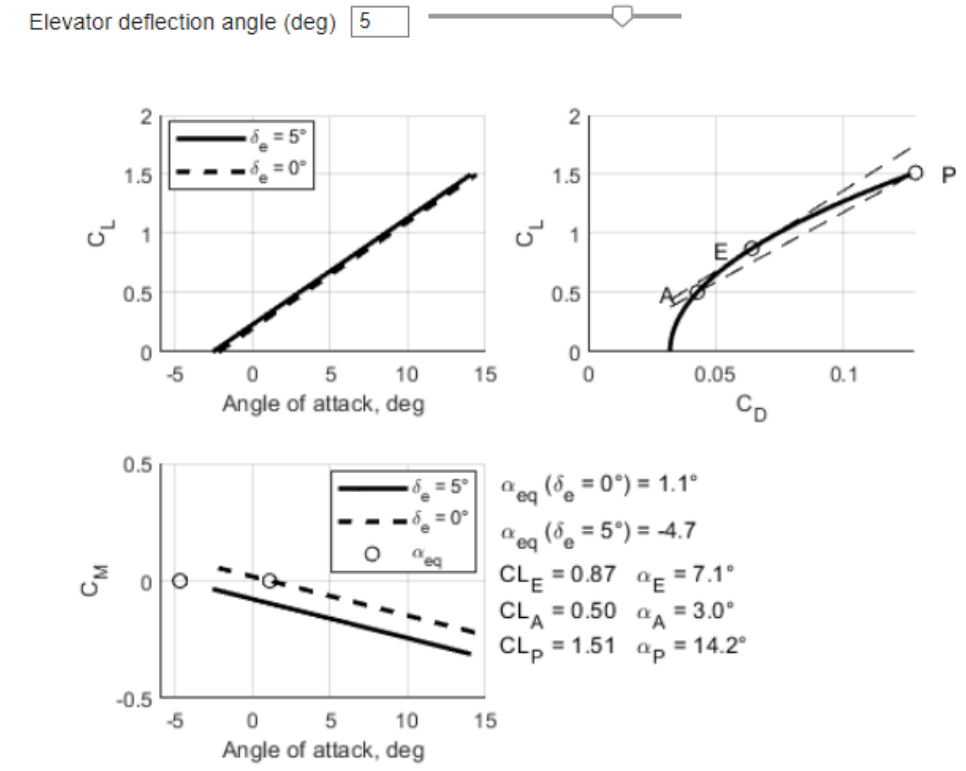

Figure 4 – Parabolic drag polar, $C_L - \alpha$ and $C_M - \alpha$ curves at $\delta_e = 5°$

Longitudinal equilibrium equations:

- $C_L = C_{L_0} + C_{L_\alpha}\alpha + C_{L_{\delta e}}\delta_e + C_{L_{i_h}} i_h;$ *(8)*
- $C_M = C_{M_0} + C_{M_\alpha}\alpha + C_{M_{\delta_e}}\delta_e + C_{M_{i_h}} i_h;$ *(9)*

From the longitudinal equilibrium equations, when the value of δ_e increases, the $C_L - \alpha$ curve moves upwards while $C_M - \alpha$ curve moves downwards and vice versa when δ_e decreases.

For fixed i_h, increasing δ_e, the value of α for a given C_L tends to decrease and the $C_L - \alpha$ curve moves up, consequently also the value of α such that $C_M = 0$ decreases and the $C_M - \alpha$ curve moves down.

2. Wing planform and its contribution to aircraft longitudinal and lateral-directional stability

2.1 Representation of wing

In this section a code is implemented for the representation of the wing in planform and in front view by varying some characteristic parameters.

It is possible to set values for:

- Aspect ratio AR
- Taper ratio λ
- Sweep Λ_{le}
- Dihedral angle Γ

Let us consider a first set of data, named wing A:

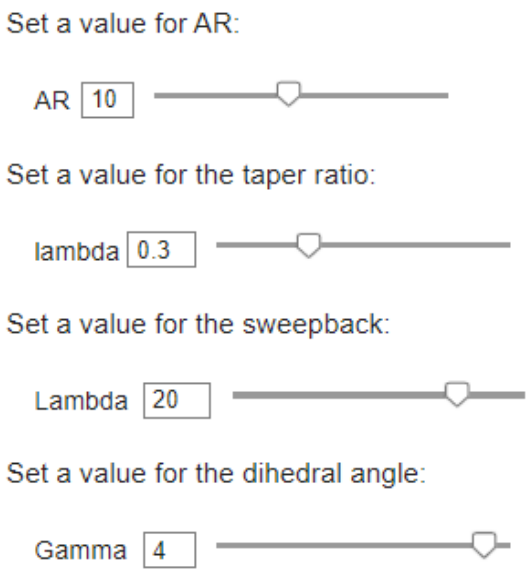

Figure 5 – Value set for the wing A

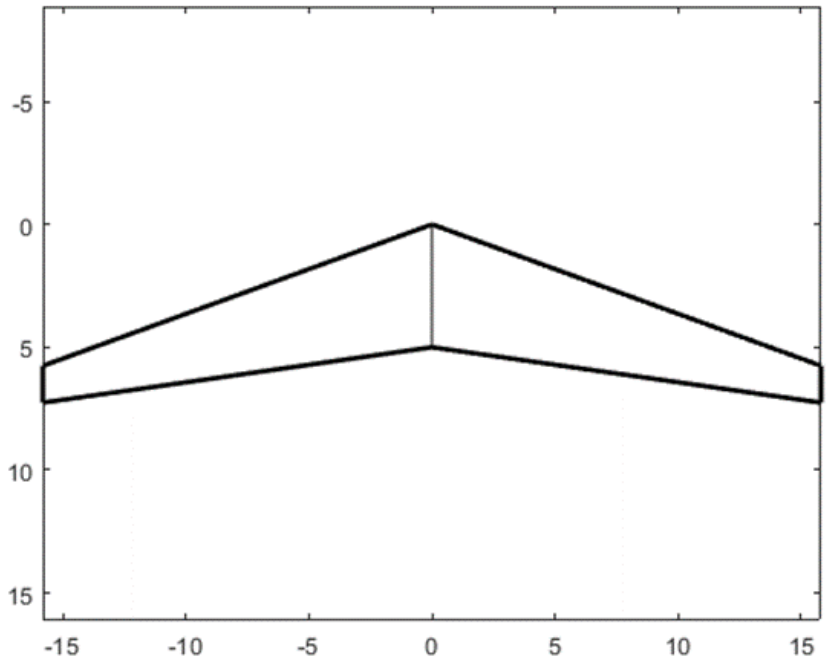

Figure 6 – Wing A in top view

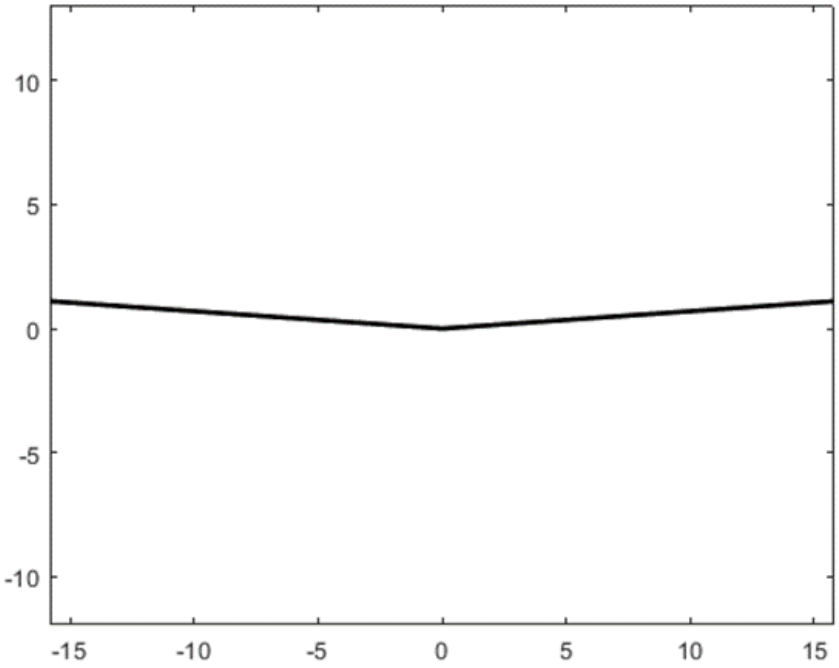

Figure 7 – Wing A in front view

Then, let us consider another planform, named wing B:

Set a value for AR:

AR 10

Set a value for the taper ratio:

lambda 0

Set a value for the sweepback:

Lambda 40

Set a value for the dihedral angle:

Gamma -5

Figure 8 – Value set for the wing B

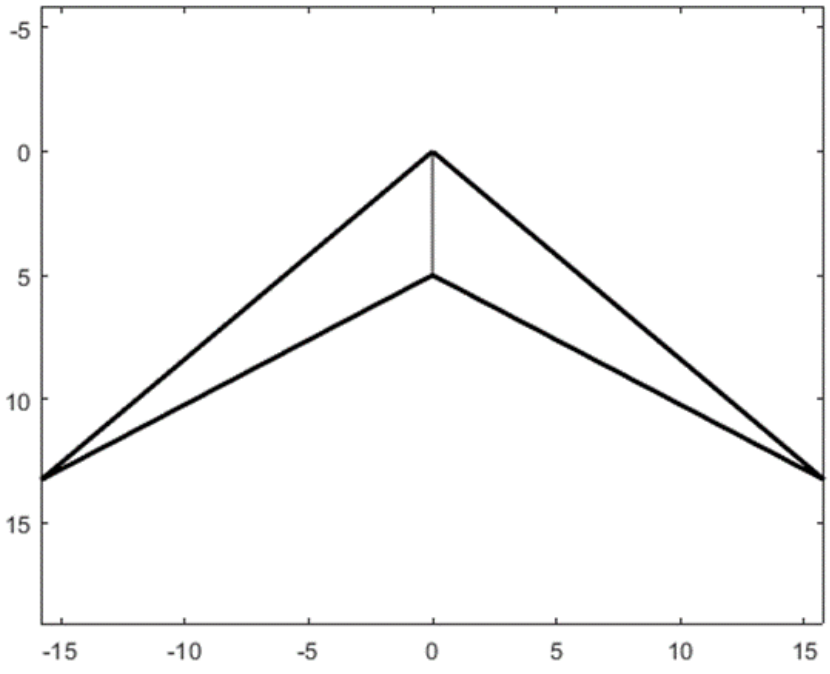

Figure 9 – Wing B in top view

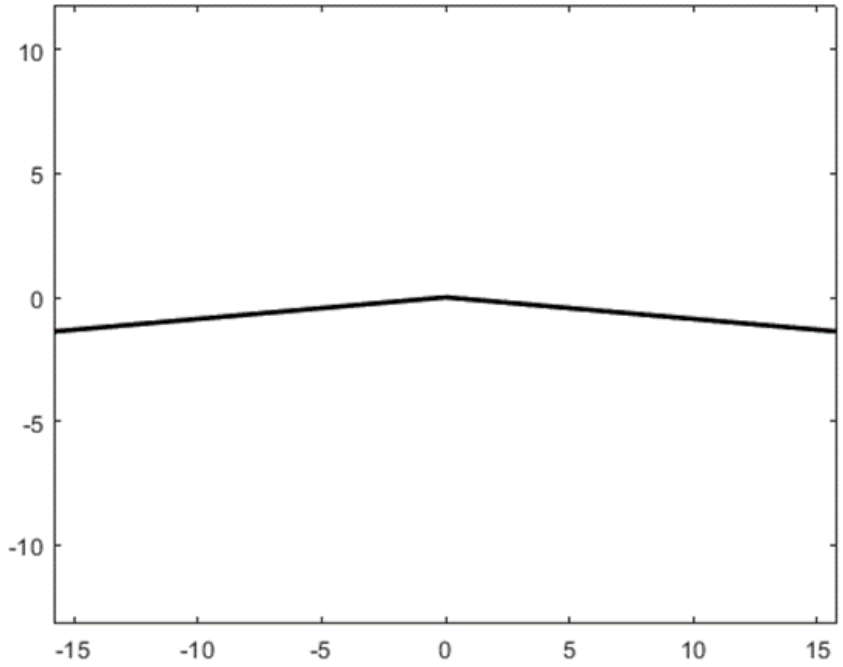

Figure 10 – Wing B in front view

2.2 Static stability coefficients

Some coefficients relating to lateral and directional stability are determined

For the wing A:

```
CN_beta = 0.020 /rad
Cl_beta_gamma = -0.376 /rad
CL_alfa,w = 5.251 /rad
Cl_beta_Lambda = -0.264 /rad
```

Figure 11 – Stability coefficients for wings A

While for the wing B:

```
CN_beta = 0.043 /rad
Cl_beta_gamma = -0.544 /rad
CL_alfa,w = 4.679 /rad
Cl_beta_Lambda = -0.328 /rad
```

Figure 12 – Stability coefficient for wings B

2.2.1 Wing pitching moment

For the evaluation of this coefficient, we can use this equation:

$$C_{M_{ac}} = C_{M_0} \cdot \left(\frac{\mathrm{AR}\cos^2(\Lambda_{le})}{\mathrm{AR} + 2 \cdot \cos(\Lambda_{le})} \right); \quad (10)$$

Equation 10 – Simplified equation for the evaluation of the wing pitching moment about the aerodynamic center

Where C_{M_0} is the airfoil pitching moment, here assumed equal to −0.06.

In this equation we can see the relationship between $C_{M_{ac}}$, AR and Λ_{le}, thus we can represent the variation of $C_{M_{ac}}$ with AR at different values of Λ_{le}.

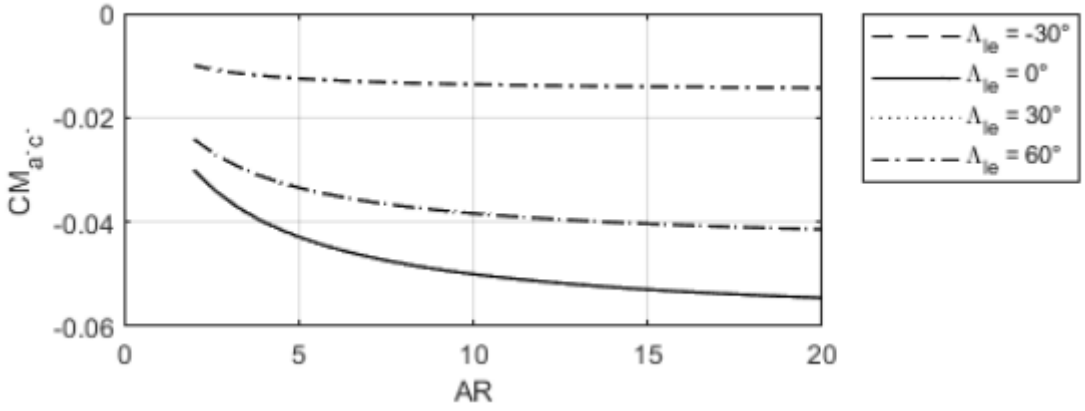

Figure 13 – $C_{M_{ac}}$-AR curves

The cosine is an even function, hence the trend of $C_{M_{ac}}$ at $\Lambda_{le} = -30^{\circ}$ and $\Lambda_{le} = 30^{\circ}$ is the same. For this reason, in the above figure the dashed and the dotted lines are overlapped.

2.2.2 Contribution of the wing due to sweep angle to the yaw moment coefficient

The contribution of the wing due to the sweepback to the yaw moment coefficient is calculated by the DATCOM method (Rif. 1) (Finck, 1978):

$$\frac{C_{N_\beta}}{C_L^2} = \frac{1}{57.3}\left[\frac{1}{4\pi AR} - \frac{\tan\left(\Lambda_{c/4}\right)}{\pi AR\left(AR + 4\cos\left(\Lambda_{c/4}\right)\right)}\left(\cos\left(\Lambda_{c/4}\right) - \frac{AR}{2} - \frac{AR^2}{8\cos\left(\Lambda_{c/4}\right)} + 6\frac{\bar{x}}{c}\left(\frac{\sin\left(\Lambda_{c/4}\right)}{4}\right)\right)\right] \quad (11)$$

Equation 11 – DATCOM method for the evaluation of the wing contribution to directional stability

where $\bar{x}$ is the longitudinal distance from the coordinate origin (usually the center of gravity) to the wing aerodynamic center.

The center of gravity is assumed to be at 25% of the root chord and the wing aerodynamic center is assumed to be at 25% of the medium aerodynamic chord $\bar{c}$.

We can assume, for the determination of C_{N_β} of the wings A and B, $C_L = 1$;

For the determination of $\Lambda_{C/4}$ we can use this equation:

$$\tan\Lambda_x = \tan\Lambda_{le} - \frac{4x(1-\lambda)}{AR(1+\lambda)} \quad (12)$$

Equation 12 – equation for the estimation of Λ_x

In which we set $x = \frac{1}{4}$;

Now from the equation of C_{N_β} we can represent the variation of this coefficient whit the C_L at different values of Λ_{le}

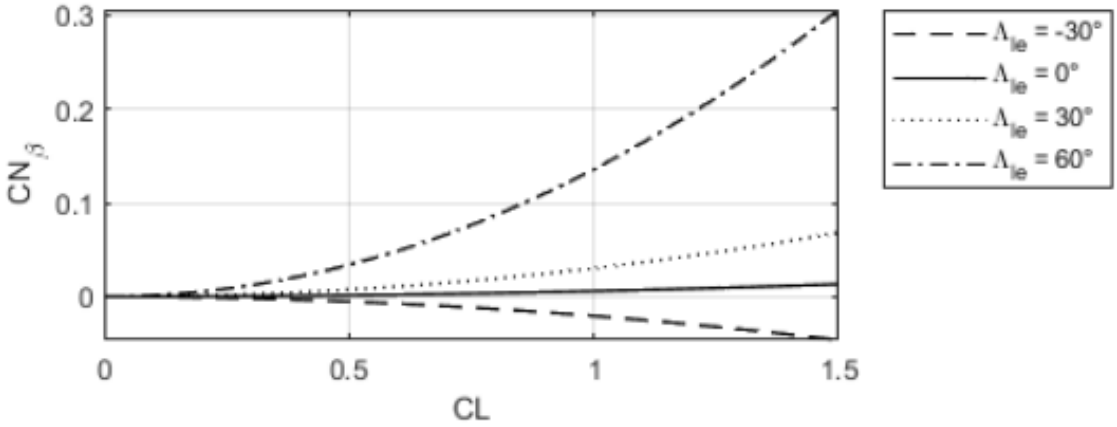

Figure 14 – C_{N_β}-C_L curves, values in rad^{-1}

From (11) and Figure 14 we can see that the trend of C_{N_β} respect to C_L is not linear, in fact C_{N_β} depends on the square of C_L.

2.2.3 Contribution of the dihedral effect to roll coefficient

In general, C_{l_β} must be negative for lateral stability. In fact, if the wind coming from the right and the aircraft rolls to the left, the lift tilts and produces a lateral force providing a lateral translation to the left, which tends to cancel the component of velocity $Vsin(\beta)$, where β is the sideslip angle. The term C_{l_β} is the contribution of the dihedral effect to the roll coefficient.

A. *The wing-fuselage contribution to the dihedral effect due to the dihedral angle*

The wing-fuselage contribution to the dihedral effect due to the dihedral angle $C_{l_{\beta,\Gamma}}$ is:

$$C_{l_{\beta,\Gamma}} = -\frac{\Gamma(\text{rad})}{6} C_{L_{\alpha,w}} \frac{1+2\lambda}{1+\lambda} \tag{13}$$

Equation 13 – $C_{l_{\beta,\Gamma}}$ equation

where $C_{L_{\alpha,w}}$ is calculated with the POLHAMUS formula ($M_\infty = 0$):

$$C_{L_{\alpha,w}} = \frac{2\pi \text{AR}}{2 + \sqrt{4 + \frac{\text{AR}^2(1-\text{M}_\infty)}{k_p^2}\left(1 + \frac{\tan^2\left(\Lambda_{c/2}\right)}{1-\text{M}_\infty^2}\right)}} \qquad k_p = \begin{cases} 1 + \text{AR}\left(\frac{1.87 - 0.000233\Lambda_{le}}{100}\right) & \text{if AR} < 4 \\ 1 + \frac{(8.2 - 2.3\Lambda_{le}) - \text{AR}(0.22 - 0.153\Lambda_{le})}{100} & \text{if AR} \geq 4 \end{cases} \tag{14}$$

Equation 14 – POLHAMUS Formula

We can represent the variation of $\boldsymbol{C_{l_{\beta,\Gamma}}}$ with $\boldsymbol{C_L}$ at some values of $\boldsymbol{\Lambda_{le}}$

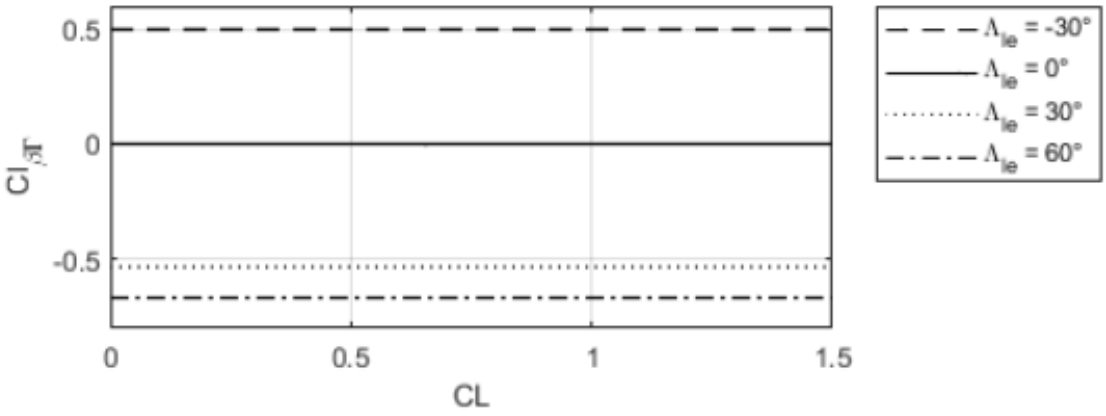

Figure 15 – $C_{l_{\beta,\Gamma}}$- C_L curves

The trend of $\boldsymbol{C_{l_{\beta,\Gamma}}}$ is constant respect to $\boldsymbol{C_L}$, in fact from (13) and (14) there is no dependence of $\boldsymbol{C_{l_{\beta,\Gamma}}}$ from $\boldsymbol{C_L}$, but from ***Figure 15*** the value of $\boldsymbol{C_{L_{\alpha,w}}}$ (hence also $\boldsymbol{C_{l_{\beta,\Gamma}}}$) depends on the value of $\boldsymbol{\Lambda_{le}}$;

We can also represent the variation of $C_{L_{\alpha,w}}$ with the aspect ratio AR at different values of Λ_{le}.

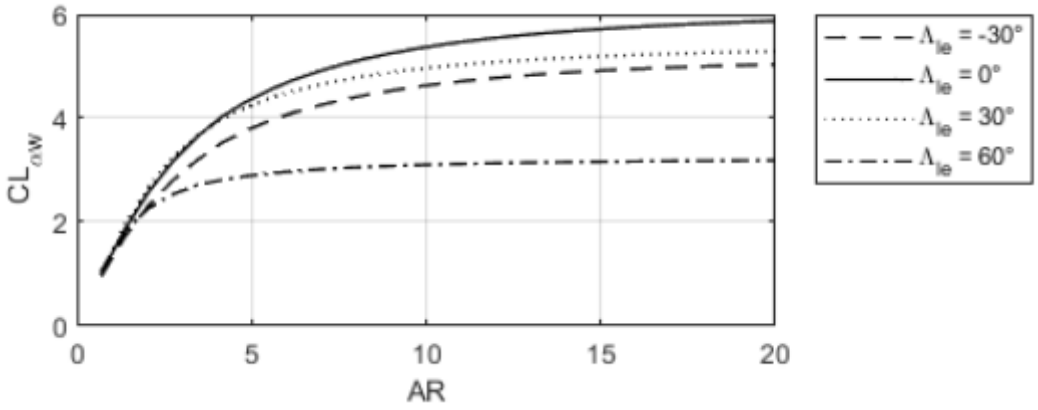

Figure 16 – $C_{L_{\alpha,w}}$ – AR curves

B. The wing-fuselage contribution to the dihedral effect due to sweep angle

The wing-fuselage contribution to the dihedral effect, due to the sweep angle, is:

$$C_{l_{\beta,\Lambda}} = -\frac{1}{3} C_L \sin(2\Lambda_{le}) \frac{1+2\lambda}{1+\lambda} \qquad (15)$$

Equation 15 – $C_{l_{\beta,\Lambda}}$ equation

We can also represent the variation of $C_{l_{\beta,\Lambda}}$ with C_L at different values of Λ_{le}

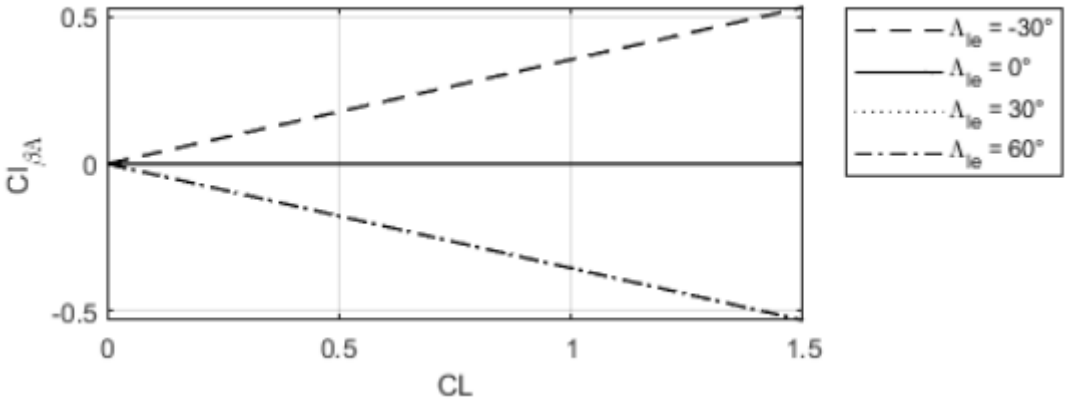

Figure 17 – $C_{l_{\beta,\Lambda}}$- C_L curves

The trend of $C_{l_{\beta,\Lambda}}$ respect to C_L is linear and the sign of the former depends on the value of Λ_{le}, in fact the sine is an odd function.

3. Introduction to range of an electric aircraft

Today's needs push more and more to the use of greener aircraft. The goal is to develop technologies, manufacturing and operational strategies providing emissions abatement. Electric propulsion is preferred for its advantages: quiet operation, higher safety, precise power management and control. (Rif. 2) (Teresa, Antonio, Luigi, Alessandro, & Marco, 187 (2017) 807-819)

Electric aircraft is just an aircraft with an alternative energy storage and propulsion system. It uses batteries for energy storage and an electric motor for propulsion.

Batteries are an alternative to the fossil fuels since no emissions are generated during flight. No combustions take place. Lithium-ion batteries currently dominate the market in electric vehicles, but when compared to the jet fuel as energy storage, the current battery technology loses its attraction.

In fact, the most important parameter is the specific energy E^* that determines how much energy can be stored per mass unit. For example, Jet-A stores about 11900 $\frac{Wh}{kg}$, while E^* of an actual battery is around 200 $\frac{Wh}{kg}$.

For regional hybrid-electric turboprop specific energies higher than 500 $\frac{Wh}{kg}$, ideally 800 $\frac{Wh}{kg}$, is needed. For an all-electric system, the required specific energy may be around 2000 $\frac{Wh}{kg}$.

A trend on specific energy derived from NASA/Boeing SUGAR study indicates that an increment of 7.6% per year is needed to achieve 750 $\frac{Wh}{kg}$ by 2030. But the fact that 750 $\frac{Wh}{kg}$ can be achieved by 2030 seems optimistic. (Rif. 3) (Danilo, et al., 2022, 9(6), 3)

In the next section we can see how to determine the range of an electric aircraft, evaluate its range in some conditions and with the variation of the following parameters:

- Battery specific energy E^*
- Lift to drag ratio $\frac{L}{D}$
- Propulsion efficiency η_{tot}
- Mass battery fraction $\frac{m_{batt}}{m}$

Then the diagram of the range R with the battery specific energy E^* is shown with the variation of the lift to drag ratio $\frac{L}{D}$;

3.1 Equation of the range of an electric aircraft

A plane spends most of its energy producing thrust. This thrust pushes the plane forwards, countering drag and producing lift as a side effect of velocity.

The maximum amount of energy that an aircraft can consume is a function of how much thrust it needs over the distance it flies.

In particular:

$$E = T \cdot d \tag{16.1}$$

- $[E](Energy) = J;$
- $[T](Trust) = N;$
- $[d](distance) = m;$

Now, consider an electric aircraft. It is just an aircraft with an alternative energy storage and propulsion system, in particular it uses batteries for energy storage and an electric motor for propulsion.

Thus, for this aircraft the energy *E* is:

$$E = E^* \cdot m_{batt} \cdot \eta_{TOT} \tag{16.2}$$

where:

- E^* is battery specific energy
- m_{batt} is battery mass
- η_{TOT} is propulsion efficiency from cell to airflow.

We can express weight W through the lift to drag ratio $\frac{L}{D}$ and then derive the thrust T;

$$W = L = D \cdot \frac{L}{D} = T \cdot \frac{L}{D} \Rightarrow T = W \cdot \frac{D}{L}; \tag{17.1}$$

hence we have:

$$W \cdot \frac{D}{L} \cdot \mathrm{d} = E^* \cdot m_{batt} \cdot \eta_{TOT}; \tag{18}$$

d is the range, let us rename it R;

thus, the range is:

$$R = \frac{E^* \cdot m_{batt} \cdot \eta_{TOT}}{W \cdot \frac{D}{L}}; \tag{19.1}$$

But $W = m \cdot g$; *(17.2)*

where:

- m is the total mass of the aircraft
- g is the acceleration of gravity

Finally, the range is:

$$R = E^* \cdot \frac{m_{batt}}{m} \cdot \frac{1}{g} \cdot \frac{L}{D} \cdot \eta_{TOT} \; ; \qquad (19.2)$$

(Rif. 4) (Lochie Ferrier, s.d.)

3.2 A script for the estimation of the range of an electric aircraft

If we set a value for the different parameters to estimate the range, we obtain a different value of the ideal range by using the equation *(13.2).*

It is implemented a program by using MATLAB LIVE SCRIPT to estimate the ideal range.

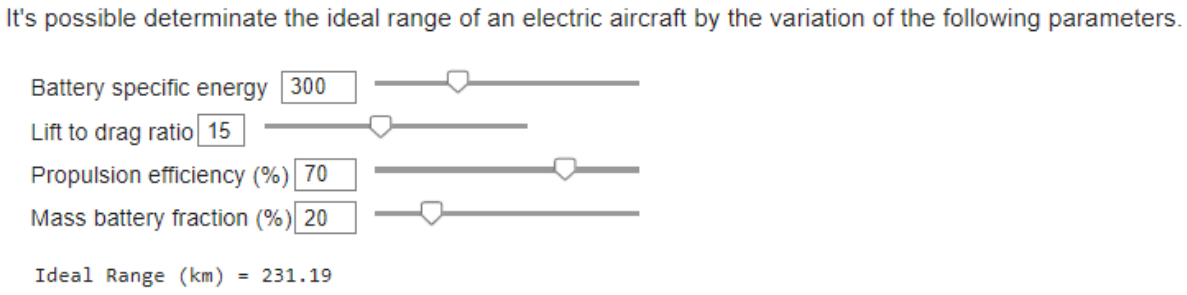

Figure 18 – Parameters for ideal range 1

Currently the value of E^* is about 300 $\frac{Wh}{kg}$ and the lift to drag ratio is limited around 35 in an optimistic view.

To increase the range, it is possible to work on E^*, or battery technology in other words, and progress seems to be moving along at 7.6% a year. That will give us the big gains over decades but won't deliver the vision right now. The lift to drag ratio $\frac{L}{D}$ is limited to around 35 by advances in aerodynamics. That's being very optimistic.

Now if we set the same value of mass battery fraction $\frac{m_{batt}}{m}$ and propulsion efficiency η_{TOT} but, in an optimistic view, we set the value of $E^*$to 1000 $\frac{Wh}{kg}$ and $\frac{L}{D}$ to 35 we can obtain the value of the ideal range in this condition, in particular:

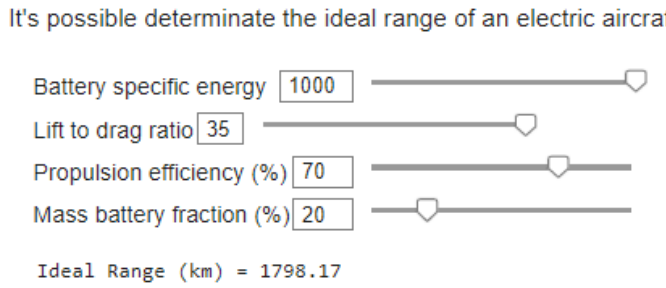

Figure 19 – Parameters for ideal range 2

Finally, if we imagine increasing the mass battery fraction $\frac{m_{batt}}{m}$ for example to 0.7, we can further increase the range. This is maybe achievable if we reduce payload capacity even on current airframes.

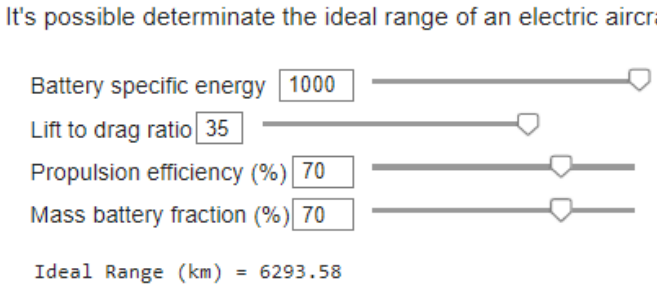

Figure 20 – Parameters for ideal range 3

3.3 Range vs. technological level of energy storage

The following diagram shows the variation of the range R with the battery specific energy E^*, by the variation of the lift to drag ratio $\frac{L}{D}$.

The value of $\frac{m_{batt}}{m}$ and η_{TOT} are the same of Figure 18.

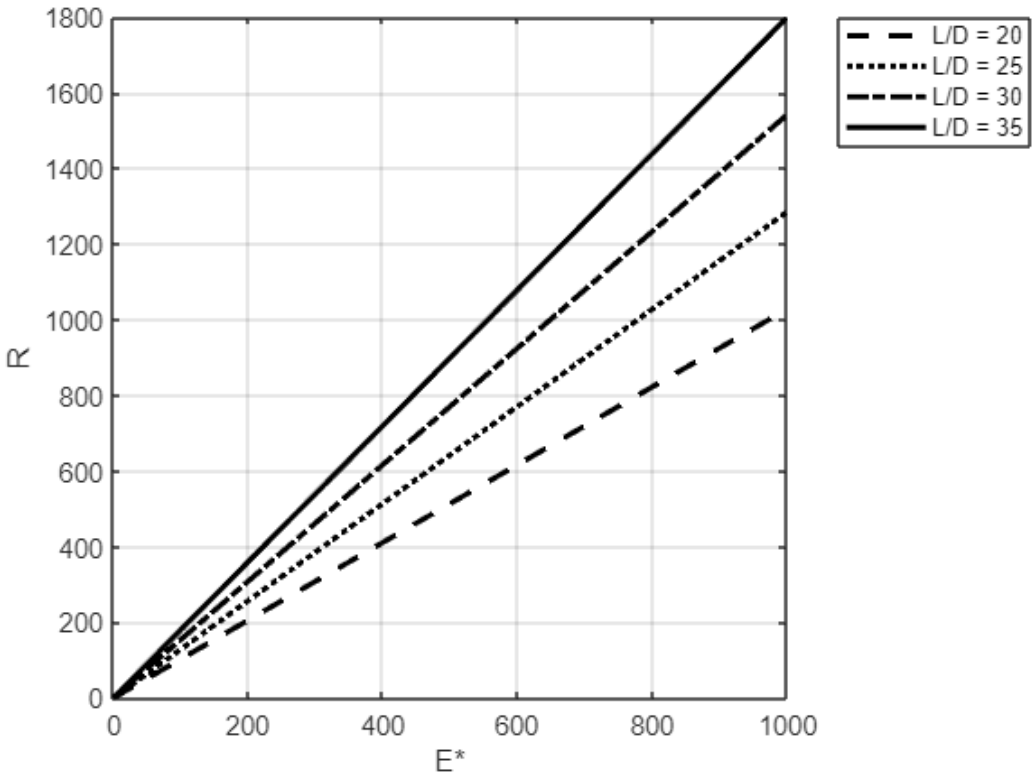

Figure 21 – R-E* curves

3.4 Considerations

We have seen that the specific energy $E^*$of modern batteries is about 300 $\frac{Wh}{kg}$. Now we can consider an aircraft powered by Jet-A fuel. The Jet-A has a lot of energy/weight. It is about 11 900 $\frac{Wh}{kg}$. If an aircraft has 27310 Kg of a Jet-A (for example the 737), it has around 325000000 Wh of Energy. If we want to reach the same energy as 27310 kg of Jet-A, 1.1 million kg of batteries are needed (it is about 13 B-737)!

We can represent the relation between the mass of batteries and mass of Jet-A in an approximate graph.

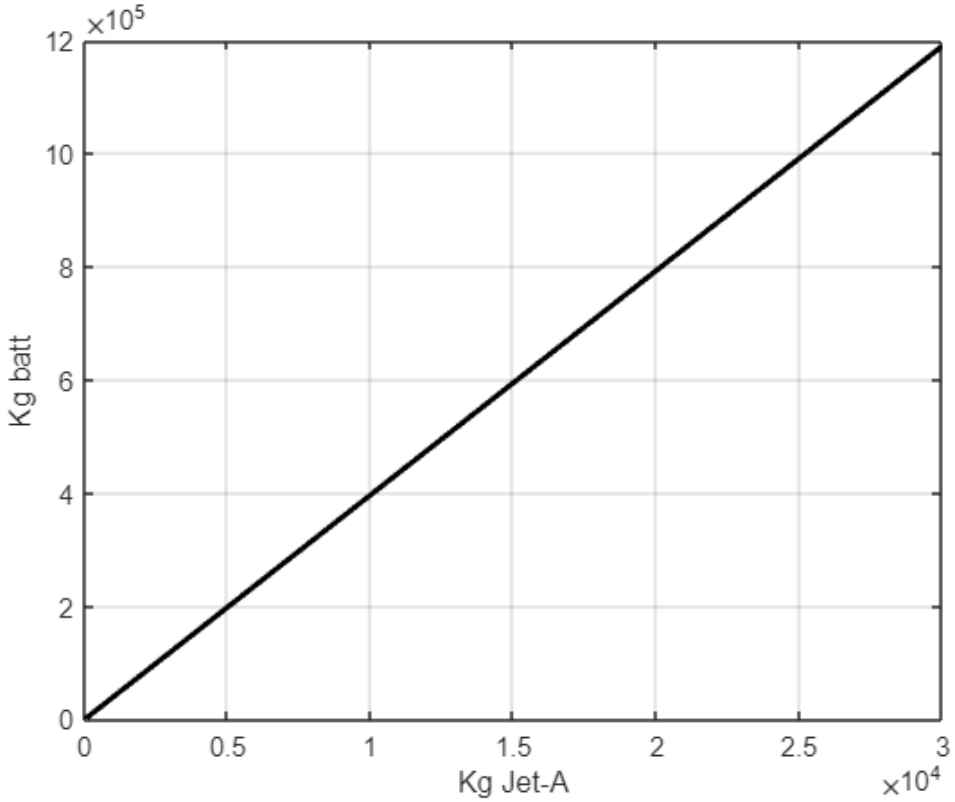

Figure 22 – Relation between kg of Jet-A and kg of batteries

This result makes us understand how the development of an electric aircraft still requires study and innovate design not only in terms of the development of electric propulsion but also in terms of the design of the entire aircraft.

Bibliografia

[1] Finck, R.D. USAF Stability and Control DATCOM; Wright-Patterson Air Force Base, Ohio, 1978

[2] Teresa Donateo, Antonio FIcarella, Luigi Spedicato, Alessandro Arista, Marco Ferraro Applied Energy 187 (2017) 807–819

[3] Danilo Ciliberti, Pierluigi Della Vecchia, Vittorio Memmolo, Fabrizio Nicolosi, Guido Wortmann, Fabrizio Ricci *Aerospace* 2022, *9*(6), 3 https://doi.org/10.3390/aerospace9060319

[4] https://lochief.wordpress.com/2015/08/04/how-the-musk-electric-jet-works/